

熊本大学学術リポジトリ

Kumamoto University Repository System

Title	Decay Kinetics of Photoinduced Solitons on a One-Dimensional Lattice with Traps
Author(s)	Tabata, Yoshinori; Kuroda, Noritaka
Citation	Journal of the Physical Society of Japan, 78(3): 034704-1-034704-7
Issue date	2009-03
Type	Journal Article
URL	http://hdl.handle.net/2298/11469
Right	© 2009 The Physical Society of Japan

Decay Kinetics of Photoinduced Solitons on a One-Dimensional Lattice with Traps

Yoshinori TABATA* and Noritaka KURODA¹

Faculty of Pharmaceutical Sciences, Hokuriku University, Kanazawa, 920-1181

¹ *Department of Materials Science and Engineering, Graduate School of Science and Technology, Kumamoto University, Kumamoto, 860-8555*

(Received 2008)

The survival probability of solitons diffusing on a one-dimensional lattice with traps is studied numerically. The solitons are assumed to collapse once they collide with one another or reach the traps. It turns out that as the density of the traps increases the decay profile tends to change into an exponential-like form from the extremely nonexponential one specific to the geminate recombination on a trap-free lattice. The randomness of the distance between adjacent traps, as well as the disorder of the intersite energy barriers for the hopping motion of solitons, functions to reduce the deviation of the decay profile from the case of the trap-free lattice. Our calculation reproduces the temperature-dependent decay profiles of the photoinduced neutral solitons observed recently in an *MX*-chain compound $\{[\text{Pt}(\text{en})_2][\text{Pt}(\text{en})_2\text{Cl}_2]\}_3(\text{CuCl}_4)_4 \cdot 12\text{H}_2\text{O}$ well. It is suggested that the traps are located at every 7 to 8 segments of the lattice and the height of energy barriers is irregular to some extent. The periodicity of the valence of Cu ions is discussed on the basis of this result.

KEYWORDS: trap, geminate recombination, one-dimensional lattice, random walk, *MX*-chain, soliton, decay, survival probability

* E-mail: y-tabata@hokuriku-u.ac.jp

1. Introduction

In conjugate polymers such as *trans*-polyacetylene^{1,2)} and quasio-one-dimensional halogen-bridged mixed-valence metal complexes which are often called *MX*-chain compounds³⁻⁵⁾, soliton and antisoliton pairs can be created by the interband optical excitation of electron-hole pairs or charge-transfer excitons. For the last several decades, the problems how unequilibrated states survive or disappear and how their distribution changes with time have attracted much attention because of their unique, nonlinear transient properties. Indeed, dynamics of nonlinear dissipation of nonequilibrium quasiparticles states is a basic, important subject of physics and chemistry.⁶⁾ Therefore many studies have been accumulated so far, particularly on the survival probability of random walkers executing the geminate coalescence on a one-dimensional medium.

Torney and McConnell (hereafter abbreviated as TM) have derived the exact solution for the first time for the diffusion-limited reaction in an infinitely long continuum medium.⁷⁾ Placing nonequilibrium particles randomly in the medium as the initial condition, TM have shown that the survival probability S of a particle is given by

$$S(\zeta) = \exp(8\zeta) \operatorname{erfc}(\sqrt{8\zeta}), \quad (1)$$

where $\operatorname{erfc} x$ signifies the complimentary error function $1 - \operatorname{erf} x$ and ζ is the dimension-less variable defined as

$$\zeta = N_0^2 D t, \quad (2)$$

with the initial density of particles N_0 , the diffusion coefficient of particles D and time t after the start of reaction. The nonlinearity of the reaction manifests itself in the fact that S depends on N_0^2 .

To take account of the hopping motion of localized particles in solids, Sasaki and Nakagawa (hereafter abbreviated as SN) have extended the stochastic theory of TM to the process on a one-dimensional, discrete medium, that is, lattice.⁸⁾ For the same initial condition as that of the TM theory SN have obtained the solution

$$S(t) = \frac{2\rho_0^2}{\pi} \int_0^{\pi/2} \frac{\cos^2 \theta \exp(-8wt \sin^2 \theta)}{\rho_0^2 + (1 - 2\rho_0) \sin^2 \theta} d\theta, \quad \rho_0 = N_0 a, \quad (3)$$

where a is the lattice constant and w is the hopping rate of a particle between consecutive lattice sites. It is worth stressing that $S(\zeta)$ of eq. (1) falls vertically at $\zeta = 0$, while $S(t)$ of eq. (3) exhibits a certain slope at $t = 0$. This is because in a continuum medium there exist particles almost contacting each other even at $t = 0$, while in a discrete medium a waiting time is needed for particles residing on consecutive sites to collide with each other. Apart from this difference in the initial behavior, the two theories yield the same the gross feature of the decay profile of nonequilibrium particles. Since proximal particle pairs react earlier than others, more isolated particles survive for a longer time. Consequently, $S(t)$ exhibits a strikingly nonexponential time evolution.

These theoretical works have been successfully applied to the interpretation of the experimental results on long-lived solitons in *MX*-chain compounds.^{9,10)} By irradiation with visible light, a midgap absorption band due to neutral solitons is generated in crystals of $[\text{Pt}(\text{en})_2][\text{Pt}(\text{en})_2\text{Cl}_2](\text{ClO}_4)_4$ and $[\text{Pt}(\text{en})_2][\text{Pt}(\text{en})_2\text{Cl}_2](\text{BF}_4)_4$, where (en) denotes ethylenediamine. The midgap band exhibits an extremely nonexponential time decay obeying eqs. (1) and (3). It lasts longer than 10 min even at room temperature. From the temperature dependence of the decay profile, the photoinduced solitons are suggested to execute a thermally activated random walk jumping over the energy barriers with the height of 0.4–0.5 eV. These large barrier height and the long life time have led Kuroda and coworkers to conceive that there might be some local disorders serving as energy barriers which physically divide Pt-Cl chains into segments and that there should be a relaxation mechanism for the photogenerated charge-transfer excitons to decompose into solitons and antisolitons separately in different segments.^{11,12)}

It has been found further that solitons may survive much longer if the energy barriers are irregular.¹¹⁾ According to a numerical simulation within the framework of the aforementioned situation of Pt-Cl chains, as the irregularity of the energy barriers evolves, S is transformed into the stretched exponential form^{12–14)}

$$S(\zeta) = \exp[-(\zeta / \zeta_{1/e})^\beta], \quad 0 < \beta < 1, \quad (4)$$

where $\zeta_{1/e}$ is a constant, in agreement with the empirical knowledge^{15–18)} that the decay

profiles of nonequilibrium states in disordered systems often have a form of the stretched exponential function. If the Gaussian distribution is assumed for the height of energy barriers, the value of the argument β decreases from 0.43 to 0.35–0.25 as the Gaussian width increases from 0 to 0.1 eV. It has been confirmed also that if β is adjusted eq. (4) reproduces the decay profiles observed for different samples of the BF_4 salt of the PtCl-chain compound very well.

Recently, a novel characteristics has been observed in another PtCl-chain compound $\{[\text{Pt}(\text{en})_2][\text{Pt}(\text{en})_2\text{Cl}_2]\}_3(\text{CuCl}_4)_4 \cdot 12\text{H}_2\text{O}$.¹⁹⁾ In this compound the decay profile of the photoinduced midgap band contains a significant amount of the exponential component. In addition, the decay rate becomes faster as temperature is elevated, so that at 150 K the midgap absorption band almost disappears at $t = 200$ s, in quite contrast to the observations in ClO_4 and BF_4 salts. It is evident that the pictures of geminate recombination, which have been mentioned hitherto, cannot explain this phenomenon, suggesting the existence of additional processes that promote extinction of solitons.

In this relation we recall that Zozulenko and his coworkers have theoretically paid attention to reactions of quasiparticles in a segment of a one-dimensional medium with absorbing traps at the ends.^{20–22)} They have derived a formula for $S(t)$ in the form of double infinite series, showing that at t satisfying $5\pi^2 wt / n^2 \gg 1$ it is asymptotically represented as

$$S(t) = \exp(-5\pi^2 wt / n^2), \quad (5)$$

where n is the segment length. Furthermore, extending this result they have shown that if traps distribute randomly in a long chain $S(t)$ changes to a stretched exponential form of $\exp[-(3/2)(10\pi^2 c^2 wt)^{1/3}]$ for $10\pi^2 c^2 wt \gg 1$, where c is the trap concentration.

In light of these works of Zozulenko and his coworkers, it is likely that traps play a crucial role in the PtCl-compound of $\text{CuCl}_4 \cdot \text{H}_2\text{O}$ salt. Unfortunately, however, in their theory a single pair of particles is put on every segment of medium as the initial condition, although from the experimental point of view the number of particles confined initially between traps should be arbitrary. Moreover, to introduce the disorder to the system Zozulenko *et al.* have postulated a chaotic distribution for the length of each segment. Such an extreme randomness is not necessarily an appropriate condition for the $\text{CuCl}_4 \cdot \text{H}_2\text{O}$ salt since the traps could be originated for some reasons relating to the crystal structure.^{23,24)} Nevertheless, to the authors'

knowledge, no studies on the collaboration between geminate recombination and trapped annihilation under arbitrary conditions have been conducted to date.

In the present work we investigate the kinetics of nonequilibrium particles on the one-dimensional lattice with traps by numerical simulation. The initial number of particles, the density of the traps and the degree of the disorder of the barrier height are chosen arbitrary. The calculation procedure is described in the next section. In §3, the dependence of the decay profile on the disorder of the arrangement of traps is studied. The results of the simulation of the experimental data and discussions about the search for optimum parameters are also presented in §3.

2. Calculation Procedure

Our numerical calculation targets the neutral solitons walking randomly on a one-dimensional lattice, jumping over the energy barriers as schematized in Fig. 1 (a). In our model, the annihilation of solitons is executed in two ways irreversibly. One of them is by geminate recombination of mutually adjoining solitons. It occurs when they come into the same segment for an instant. Then, a pair of solitons is removed immediately from the segment. The other is by traps, which are set uniformly or randomly on the lattice. The trap captures the soliton and removes it instantaneously from the chain, even if it is a single unpaired soliton, when the soliton enters the site with a trap. The removal of an unpaired soliton by traps does not disarrange the phase of the order of solitons and antisolitons because there is no distinction between a soliton and an antisoliton originally if they are neutral solitons. Hence, the consecutive pair recombination is not disturbed by this removal.

In a real crystal, a segment consists of one or more lattice sites, if the energy barrier originates in defects. However, here, we treat one segment as one lattice site since a soliton is considered to move very rapidly in a segment compared with its velocity that is controlled by energy barriers and there exists no essential difference in calculation. In this case, the energy barrier is put at each intersite of the lattice as illustrated in Fig. 1 (b). In an argument on the kinetics of solitons, this treatment does not cause loss of generality. It reduces the computation time and is expected to actualize the local properties of the lattice. Here, we are noting for the following discussion that one or more segments exist in a region between adjacent traps on the lattice.

The simulation is carried out with respect to a lattice ring comprised of 10^5 sites as the standard model and it is elongated to 10^7 sites if necessary.

In order to handle the lattice with a disorder, we introduce the Gaussian distribution with the width of σ onto the height E of the energy barrier as follows:

$$g(E) = \frac{1}{\sigma\sqrt{2\pi}} e^{-\frac{(E-E_0)^2}{2\sigma^2}}, \quad 0 \leq \sigma \leq E_0, \quad (6)$$

where E_0 is the mean height of E .

Solitons hop from a site to neighboring sites across the barriers at the rate

$$w = w_0 e^{-\frac{E}{kT}}, \quad (7)$$

where w_0 , k and T denote the hopping rate constant, Boltzmann constant and temperature, respectively. For $\sigma = 0$, this equation gives the diffusion coefficient as

$$D = D_0 = a^2 w_0 e^{-\frac{E_0}{kT}}, \quad (8)$$

where a is the lattice constant.

Initially, assuming photogeneration of solitons, an even number of solitons are distributed at random on the sites of the chain on the basis of binomial occupation. However, the condition of an even number is not very important in the present model where an unpaired soliton is eliminated.

In this computation, there is arbitrariness in setting the value of either E_0 or T since the hopping rate w is determined only by the ratio E_0/T in the present model, as is obvious by eq. (7), if σ and w_0 are kept constant and T remains in the range where the energy barrier can limit the kinetics of solitons. We fix E_0 and w_0 at 0.4 eV and 10^6 step⁻¹, respectively, as in the previous simulation.¹²⁻¹⁴⁾ The value of E_0 has been adopted based on the experimental studies.^{9,11)} Then, we treat E_0/T as a calculation parameter and write it as $(E_0/T)_{\text{(cal)}}$.

3. Result and Discussion

3.1 Effect of trap

Figures 2 (a) and (b) show typical simulated decay curves at 200, 240 and 300 K as functions of ζ for the cases of uniformly arranged traps and randomly distributed ones, respectively. Here, the trap density to the number of lattice sites is set to be 0.1 and the initial density of solitons is selected to be 0.02.

In each figure, the curve labeled SN is the survival probability on an ordered trap-free lattice, for comparison. When particles repeat arbitrary hopping to the right or left nearest neighbor site on a one-dimensional ordered lattice, the probability that any of the particles meets another particle and results in pair annihilation is proportional to N_0^2 and D_0 . Hence, SN converges on a single curve independent of N_0 and T if it is scaled by ζ .

The survival probability on a disordered lattice (labeled $\sigma = 0.05$ eV) with traps decreases faster than that given by SN. It is considered that this fast decay is caused with the trap, because the soliton survives much longer when the irregularity of barriers increases on a trap-free lattice. The mean diffusion coefficient of this disordered lattice is estimated to be $D_0 \exp[(\sigma/kT)^2/2]$. The increase of the mean diffusion coefficient with elevating temperature is reduced due to the factor $\exp[(\sigma/kT)^2/2]$ that decreases by an order of magnitude upon the temperature change from 200 K to 300 K. The spreading of these curves is caused by this reduction, regardless of the existence of traps.

For an ordered lattice (labeled $\sigma = 0$ eV), the decay curves converge on a single curve, although the traps exist. The survival probability on an ordered lattice decreases further faster than that on a disordered lattice. In particular, it is notable that these decay curves seem to approach an exponential-like form by introducing the uniformly arranged traps. On the contrary, the randomly distributed traps do not transform the decay form into an exponential-like one. Additionally, the uniformly arranged traps contribute to the decay more than the randomly located ones.

In order to quantify the similarity of simulated $S(t)$ to an exponential form, we have obtained the best fit of the stretched exponential function $s(t) = \exp[-(t/\tau_{1/e})^\beta]$ to the simulated $S(t)$ at 300 K. The value of β indicates the similarity. This fit is not highly accurate in the region of small density of randomly distributed traps. Nevertheless, it is simple and practically useful for our purpose.

Figure 3 (a) shows β and the $1/e$ decay time $\tau_{1/e}$ (steps in computation) as

functions of trap density for ordered lattices with uniformly and randomly located traps. For the case of uniformly arranged traps, as the trap density approaches 0.5, β_{uniform} (closed circles) asymptotically approaches unity, although the trap density of 0.5 is an unreal value. This signifies that the decay curve is transformed from the SN form to an exponential one and that exponential-like decay is possible in this case. On the contrary, β_{random} (open circles) for the randomly distributed traps remains ≈ 0.6 . In this case, solitons of various lifetimes coexist, because the distance between traps is various. Accordingly, the decay curve does not approach an exponential form.

The value τ_{1/e_random} (open squares) for the randomly distributed traps is larger than $\tau_{1/e_uniform}$ (closed squares) for the uniform arrangement of traps particularly at small trap density. The reason for this is that in a random distribution of traps, wide and narrow intervals are allowed between traps. The solitons located between widely separated traps will exhibit a decay profile which is similar to the SN curve, whereas the solitons located between closely spaced traps will disappear more quickly. Conversely, for a uniform distribution of traps, as the traps capture solitons at the same rate throughout the lattice, they reduce the curvature of the nonexponential SN curve. Therefore, $\tau_{1/e_uniform}$ is smaller than τ_{1/e_random} . This implies that in the case of uniformly arranged traps, the solitons cannot survive for a longer time than that in the case of randomly distributed traps.

Figure 3 (b) shows β and $\tau_{1/e}$ for a disordered lattice of $\sigma = 0.02$ eV with traps. The curve of β_{uniform} (closed circles) indicates that the transformation of the decay to an exponential form is reduced by the disorder even if the trap distribution is uniform. Further, β_{random} (open circles) for randomly distributed traps is reduced to some extent by the disorder, although its dependency on the trap density is similar to the case of an ordered lattice.

3.2 Comparison with experiment

Here, we introduce a certain index in order to quantitatively evaluate the extent to which a simulated decay curve approaches or is congruent with the experimental decay one, paying attention to the difference between the areas of the regions which are encircled with the respective decay curves and the axes of a Cartesian coordinates of t and $S(t)$. We call it ‘‘congruity’’ expediently, though the difference of the areas rather signifies the dissimilarity. The smaller the congruity is, the larger the level of congruence is. The area of the region is calculated by employing quadrature by parts. Furthermore, we introduce a conversion ratio r

(s/step) of a simulation step to the real time as a parameter in order to attain the best congruity. When we seek the best conversion ratio r that minimizes the congruity, it is necessary to minimize the difference in these areas at each temperature at the same value of r . Hence, we define the congruity as the least square sum of the difference in the areas of these curves at each temperature. The best value of r is sought scanning the calculation parameters of $(E_0/T)_{(\text{cal})}$, σ , N_0 and the trap period through trial and error. The trap period is the inverse of the trap density converted to an integer.

The novel time decay profile of the photoinduced midgap band recently observed in $\{\text{Pt}(\text{en})_2[\text{Pt}(\text{en})_2\text{Cl}_2]\}_3(\text{CuCl}_4)_4 \cdot 12\text{H}_2\text{O}$,¹⁹⁾ which is mentioned in §1, is indicated with markers in Figs. 4 (a) and (b) for 110–135 K and 140–150 K, respectively. Because it has been presented that the thermal activation energy of excited states in this complex changes at about $T_a = 136$ K by the measurement of temperature dependence of a decay of the midgap states,¹⁹⁾ the temperature is divided into two ranges on the boundary of T_a in these figures. This report has suggested that this change is not due to the structural phase transition.

As the consequence of calculation, the uniform arrangement of traps is applied and the random distribution is rejected. The optimum values of the calculation parameters that yield the least congruity are listed in Tables I and II for $T < T_a$ and $T > T_a$, respectively. Figure 5 shows the congruity as a function of the trap period for both $T < T_a$ and $T > T_a$, where the optimum values listed in Tables I and II have been used. From this figure, it appears that the traps exist at every 7 or 8 sites along the lattice chain in the temperature ranges of $T > T_a$ and $T < T_a$, respectively. However, it is considered that this difference in the periodicities of traps between $T < T_a$ and $T > T_a$ is not intrinsic to the lattice but arises due to the error margin of the experimental data, since it is noisy for $T < T_a$ and is few for $T > T_a$. Adopting 8 sites as the trap period for both temperature ranges, the simulated survival probability $S(t)$ that best reproduces the experimental result at each temperature is given by the solid lines in Figs. 4 (a) and (b).

The decay profile of the photoinduced midgap illustrated in Figs. 4 (a) and (b) seems to exhibit an exponential-like form and to approach even zero owing to a significant amount of the exponential components. These features are reproduced well by the simulated $S(t)$. The fitting parameters β and $\tau_{1/e}$ to the reproduced curve at each temperature are listed in Tables I and II. Here, $\tau_{1/e}$ is converted to the real time by multiplying it by r . β and $\tau_{1/e}$

are also presented in Fig. 6 as functions of $1/T$. The temperature dependence of β is small as the factor $\exp[(\sigma/kT)^2/2]$ of the mean diffusion coefficient $D_0 \exp[(\sigma/kT)^2/2]$ only doubles on changing the temperature from 110 K to 135 K and it is smaller from 140 K to 150 K. The mean value of β is 0.76 for $T < T_a$ and 0.84 for $T > T_a$. Further, the lattice irregularity σ is 0.02 eV for $T < T_a$ and 0.005 eV for $T > T_a$ as a result of the optimization.

The value of $\zeta_{1/e}$ is 0.195 regardless of N_0 and T in SM or TM. Since the optimal value of N_0 is a constant, the Arrhenius plot of $\tau_{1/e}$ ($= N_0^{-2} D^{-1} \zeta_{1/e}$) yields the mean height of the energy barriers E_0 , which is estimated at 0.10 eV for $T < T_a$ and 0.24 eV for $T > T_a$ from the slope of the fitting lines to $\tau_{1/e}$ as illustrated in Fig. 6. These very well reproduce the corresponding experimental values of 0.11 eV and 0.23 eV reported in ref. 19, although the intersection of two fitting lines, which indicate the temperature at which E_0 changes, shifts lower by about 5 K compared with the experiment.

There remains slightly a tendency to decay fast at an early stage and to decay slowly at a later stage in the reproduced decay curve compared with the experimental one. However, it is considered that this tendency is reduced if the accuracy of the experimental data is higher.

A segment corresponds to a lattice site in our model. Therefore, it should be said that traps are located periodically at 7 to 8 segments as for the calculation result. The removal of solitons by traps can be interpreted as follows: The lattice is substantially subdivided into short lattices at the sites with traps and solitons are eliminated at the cutting edges of the shortened lattices. We call a piece of this shortened lattice a fragment here in order to distinguish it from the segment which is a lattice area partitioned by energy barriers. Accordingly, to set the traps at every 7 to 8 segments is equivalent to chopping the lattice into short fragments that consist of segments of the same number.

From the fact that the periodically arranged traps can reproduce the experimental result well, it is natural to consider that traps are generated due to some aspect related to the periodicity of *MX*-chain structure.

The crystal structure of the $\text{CuCl}_4 \cdot \text{H}_2\text{O}$ salt consists of double one-dimensional chains called the main chain and the sub chain. The former is composed of the halogen-bridged $[\text{Pt}^{\text{II}}(\text{en})_2]$ and $[\text{Pt}^{\text{IV}}(\text{en})_2]$ units which are alternately stacked and the later, the halogen-bridged $\text{Cu}[\text{I}]$ units.^{23,24)} Because the composition of the main chain is similar to ClO_4 and BF_4 salts, it is expected that halogen ions that bridge Pt atoms are displaced from the center point of the Pt

atoms, forming a CDW state, and kinks are generated at the boundaries of twofold degenerated states; the photogenerated state is expected to be a solitonic kink. In fact, by ESR measurement, it has been confirmed to be consistent with the neutral solitons originated in Pt^{III} of the $\text{ClO}_4 \cdot \text{H}_2\text{O}$ salt.^{23,24)}

A sub chain is peculiar to the $\text{CuCl}_4 \cdot \text{H}_2\text{O}$ salt. It has been pointed out in the refs. 23 and 24 that a sub chain queues up parallel to the main chain in the phase in which a Pt atom in the main chain and a Cu atom in the sub chain are opposite to a Cl^- ion of the mutually opposed chains; in a sub chain, the valence transition of some $\text{Cu}[\text{I}]$ ions into $\text{Cu}[\text{II}]$ ions has been detected by ESR measurement. Though the place where the paramagnetic $\text{Cu}[\text{II}]$ ion exists in a sub chain is not clarified, it is considered that it may function as a trap to eliminate the random-walking solitons in the main chain due to some reason. This possibility is enhanced by the report that the creation of solitons of Pt^{III} is controllable by adjusting $\text{Cu}[\text{II}]$ ions in the counterion.^{23,24)}

If the elimination is due to the paramagnetic ion, it chops the main chain and/or the sub chain into short fragments. Our result strongly suggests the periodicity. However, the number of lattice sites included in a segment is not necessarily uniform. If the periodicity of the crystal structure is reflected in the distribution of the paramagnetic ions, it is supposed that the distance between the adjacent paramagnetic ions is uniform. It makes the number of lattice sites included in a segment uniform, because the fragments consist of the segments of the same number.

The more discussion for the origin of the tarp is further issues that need to be addressed because information for this problem is hardly provided for us until now.

This chopping the lattice into fragments does not contradict the long-range order of the lattice chain having a periodic structure.

The trap density is 0.125 if the trap period comprises 8 sites. It is larger than the soliton density, which is selected to be 0.02 as the optimum initial condition. This implies that the probability of the elimination of solitons by traps is predominant compared with that by pair annihilation. However, the process of pair annihilation is not weakened in this condition and still contributes to the decay. It is confirmed from the fact that the computation result changes and the reproducibility degrades when $(E_0/T)_{(\text{cal})}$ and σ vary from the above values.

4. Conclusions

In conclusion, we have numerically investigated the composite decay of diffusion-controlled nonequilibrium neutral solitons on a one-dimensional lattice. The composite decay involves the elimination of unpaired solitons by traps and the geminate recombination of solitons. As the density of traps increases, the decay profile approaches an exponential-like form from the extremely nonexponential one specific to the geminate recombination on a trap-free lattice. The randomness in the trap period, as well as the disorder of the intersite energy barriers for hopping motion of solitons, reduces this change of the decay profile.

Unprecedented exponential-like time decay of the photoinduced neutral solitons observed in $\{[\text{Pt}(\text{en})_2][\text{Pt}(\text{en})_2\text{Cl}_2]\}_3(\text{CuCl}_4)_4 \cdot 12\text{H}_2\text{O}$ is reproduced adequately for all measured temperature range by applying our model in which traps are arranged periodically and some irregularity is introduced in the energy barrier, without losing the information of the change of the thermal activation energy contained in the experimental data. The periodicity of the electronic structure and the lattice irregularity of this complex are discussed on the bases of the prediction made by optimization.

Acknowledgments

One of the authors (Y.T.) thanks Mr. H. Murakami for helpful discussion and kindly providing him the experimental data on the photoinduced midgap absorption band in $\{[\text{Pt}(\text{en})_2][\text{Pt}(\text{en})_2\text{Cl}_2]\}_3(\text{CuCl}_4)_4 \cdot 12\text{H}_2\text{O}$. He is also grateful to Messrs. K. Nyu and T. Kuwayama for valuable discussions about dynamic properties of solitons in *MX*-chain compounds.

- 1) Z. Vardeny, J. Strait, D. Moses, T. -C. Chung and A. J. Heeger: Phys. Rev. Lett. **49** (1982) 1657.
- 2) C. V. Shank, R. Yen, R. L. Folk, J. Orenstein and G. L. Baker: Phys. Rev. Lett. **49** (1982) 1660.
- 3) Y. Onodera: J. Phys. Soc. Jpn. **56** (1987) 250.
- 4) N. Kuroda, M. Sakai, Y. Nishina, T. Tanaka and S. Kurita, Phys. Rev. Lett. **58** (1987) 2212.
- 5) N. Kuroda, M. Ito, Y. Nishina, A. Kawamori, Y. Koderu and T. Matsukawa: Phys. Rev. B **48** (1993) 4245.
- 6) *Nonequilibrium Statistical Mechanics in One Dimension*, ed. V. Privman (Cambridge University Press, Cambridge, 1997).
- 7) D. C. Torney and H. M. McConnell: J. Phys. Chem. **87** (1983) 1941.
- 8) K. Sasaki and T. Nakagawa: J. Phys. Soc. Jpn. **69** (2000) 1341.
- 9) N. Kuroda, Y. Tabata, M. Nishida and M. Yamashita: Phys. Rev. B **59** (1999) 12973.
- 10) N. Kuroda, M. Nishida, Y. Tabata, Y. Wakabayashi and K. Sasaki: Phys. Rev. B **61** (1999) 11217.
- 11) N. Kuroda, Y. Wakabayashi, M. Nishida, N. Wakabayashi, M. Yamashita and N. Matsushita: Phys. Rev. Lett. **29** (1997) 2510.
- 12) Y. Tabata and N. Kuroda: Phys. Rev. B **61** (2000) 3085.
- 13) Y. Tabata and N. Kuroda: Synth. Met. **101** (1999) 329.
- 14) Y. Tabata and N. Kuroda: Prog. Theor. Phys. Suppl. **138** (2000) 584.
- 15) G. Zumofen, A. Blumen and J. Klafter: J. Chem. Phys. **82** (1985) 3198.
- 16) R. Saito and K. Murayama: Solid State Commun. **63** (1987) 625.
- 17) H. Scher, M. F. Shlesinger and T. J. Bendler: Physics Today **44** (1991) 26.
- 18) N. Ookubo: J. Appl. Phys. **74** (1993) 6375.
- 19) H. Murakami: Master Thesis, Graduate School of Science and Technology, Kumamoto University, Kumamoto, Japan (2006) [in Japanese].
- 20) Yu. B. Gaididel, A. I. Onipiko and I. V. Zozulenko: Phys. Lett. A **132** (1988) 329.
- 21) I. V. Zozulenko: Solid State Commun. **76** (1990) 1035.
- 22) I. V. Zozulenko: J. Phys.: Condens. Matter **5** (1993) 3611.
- 23) M. Yamashita, H. Aso, S. Matsunaga, K. Takizawa, K. Nakata, C. Kachi-Terajima, F. Iwahori, T. Ishii, H. Miyasaka, K. Sugiura, T. Kawashima, K. Takai, N. Kuroda, M. Shiro, H. Kishida, H. Okamoto, H. Takahashi, H. Tanaka, K. Marumoto and S. Kuroda: Chem. Lett. **32** (2003) 278.

- 24) H. Aso, T. Manabe, T. Kawashima, T. Ishii, H. Miyasaka, H. Matsuzaka, M. Yamashita, Hasanudin, N. Kuroda and M. Shiro: *Mol. Cryst. Liq. Cryst.* **376** (2002) 7.

Fig. 1. (a) A schematic representation of an MX -chain lattice with local disorders and traps. (b) The model of a disordered linear lattice chain with traps employed for calculation. E_0 and a denote the mean height of energy barriers and the lattice constant, respectively. The lattice area partitioned by adjacent energy barriers is the segment and the area subdivided by adjacent traps is the fragment.

Fig. 2. Examples of simulated decay curves as functions of ζ with temperature variation on a lattice with (a) uniform trap distribution and (b) random trap distribution. SN indicates the decay on an ordered lattice without traps, for comparison. Three curves labeled $\sigma = 0.05$ eV are the decays on a disordered lattice with traps. The lowest curves labeled $\sigma = 0$ eV which overlap and result in a single curve are the decays on an ordered lattice with traps. The trap density to the number of lattice sites is 0.1 here.

Fig. 3. The similarity of the simulated survival probability $S(t)$ to an exponential form expressed with β for (a) the ordered lattice and (b) the disordered lattice. $\tau_{1/e}$ denotes the $1/e$ decay time (steps in computation). The suffixes “uniform” and “random” symbolize uniformly and randomly distributed traps, respectively. The broken lines are guides for the eye.

Fig. 4. The time decay profile of solitons in $\{[\text{Pt}(\text{en})_2][\text{Pt}(\text{en})_2\text{Cl}_2]\}_3(\text{CuCl}_4)_4 \cdot 12\text{H}_2\text{O}$ obtained experimentally (markers) and that reproduced by the simulation (solid lines) for (a) $T < T_a$ and (b) $T > T_a$. Here, the trap period is chosen to 8 sites.

Fig. 5. The degree of congruence of the simulated decay curve to the experimental one as a function of the trap period (at every n sites). The smaller “Congruity” is, the larger the degree of congruence is. The broken lines are guides for the eye.

Fig. 6. The temperature dependence of the fitting parameters β ($\blacktriangledown, \blacktriangle$) and $\tau_{1/e}$ ($\blacksquare, \blacklozenge$) of the stretched exponential function $s(t) = \exp[-(t/\tau_{1/e})^\beta]$ to the reproduced $S(t)$ curve. β is expressed with a linear scale; whereas $\tau_{1/e}$, with a log scale. E_0 denotes the mean height of the energy barriers obtained from the slope of the fitting lines to $\tau_{1/e}$, which changes the

value at T_a .

Table I. Optimum calculation parameters for $T < T_a$.

T denotes the temperature at which the experiment have been conducted. $(E_0/T)_{\text{(cal)}}$ is a calculation parameter that decides the hopping rate w . β and $\tau_{1/e}$ are fitting parameters of a stretched exponential function $s(t) = \exp[-(t/\tau_{1/e})^\beta]$ to the simulated decay curve at T . r denotes the conversion ratio of a simulation step to the real time. σ and N_0 are calculation parameters, which are the lattice irregularity and the initial density of solitons, respectively. $\tau_{1/e}$ is converted to the real time by multiplying it by r here.

T (K)	$(E_0/T)_{\text{(cal)}}$ (eV/K)	β	$\tau_{1/e}$ (s)
110	1.42×10^{-3}	0.753	1416
120	1.35×10^{-3}	0.748	570
125	1.31×10^{-3}	0.765	379
130	1.28×10^{-3}	0.778	253
135	1.25×10^{-3}	0.778	181

$r = 7.95$ s/step, $\sigma = 0.02$ eV, $N_0 = 0.02$.

Table II. Optimum calculation parameters for $T > T_a$.

Refer to Table I for the display items.

T (K)	$(E_0/T)_{\text{(cal)}}$ (eV/K)	β	$\tau_{1/e}$ (s)
140	1.34×10^{-3}	0.856	61
145	1.28×10^{-3}	0.837	28
150	1.24×10^{-3}	0.829	16

$r = 1.59$ s/step, $\sigma = 0.005$ eV, $N_0 = 0.02$.

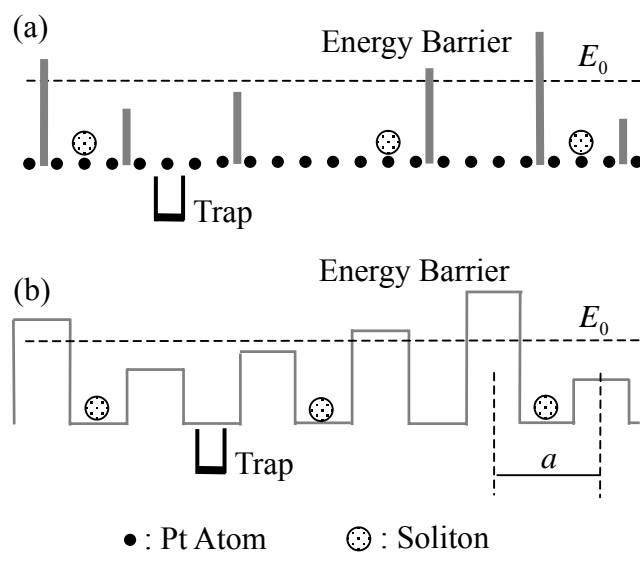


Fig. 1

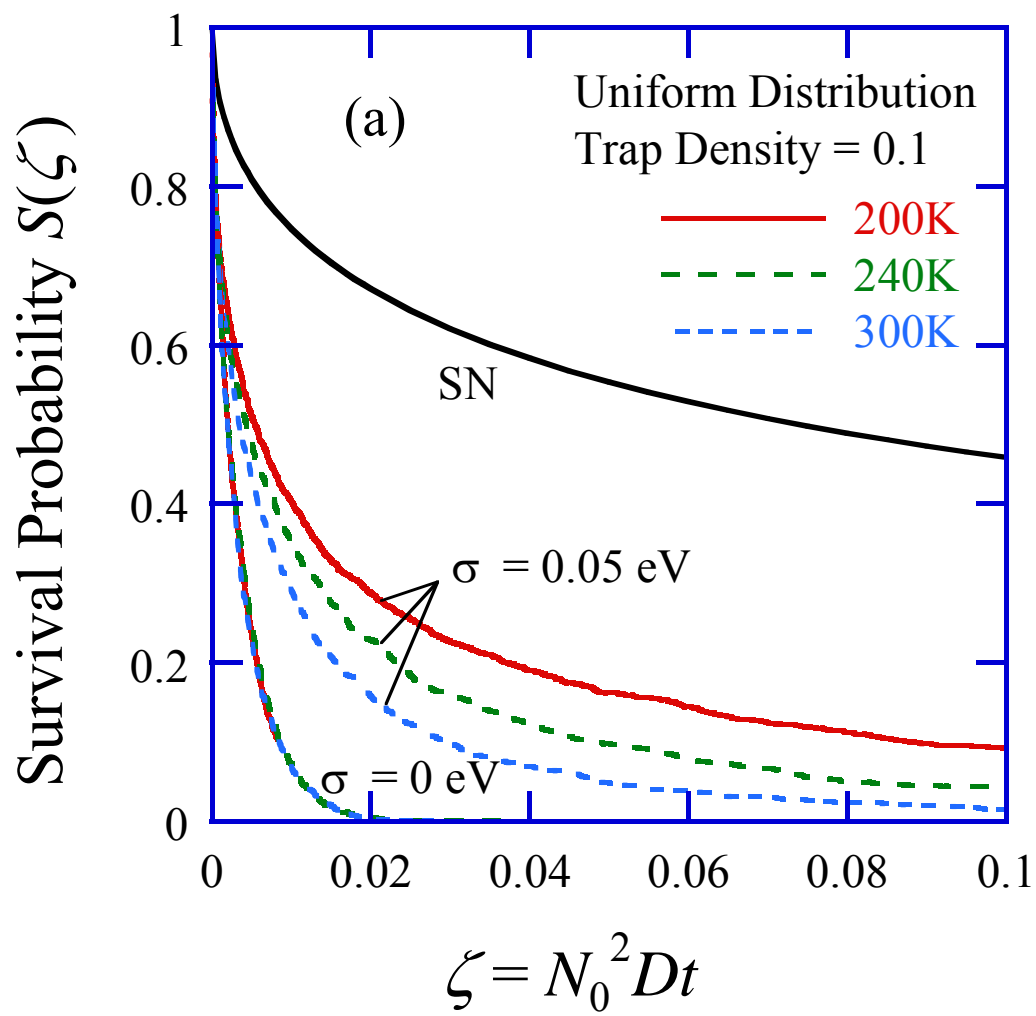


Fig. 2 (a)

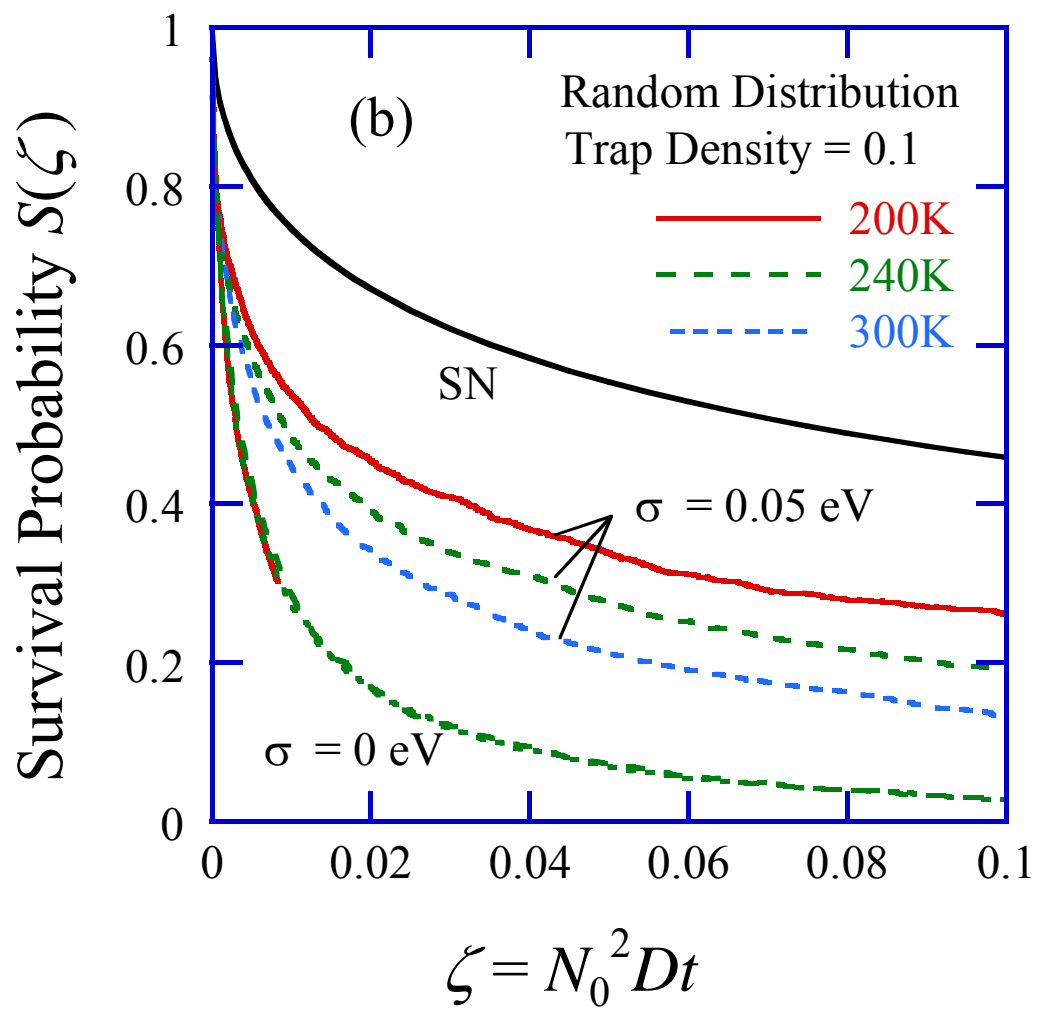


Fig. 2 (b).

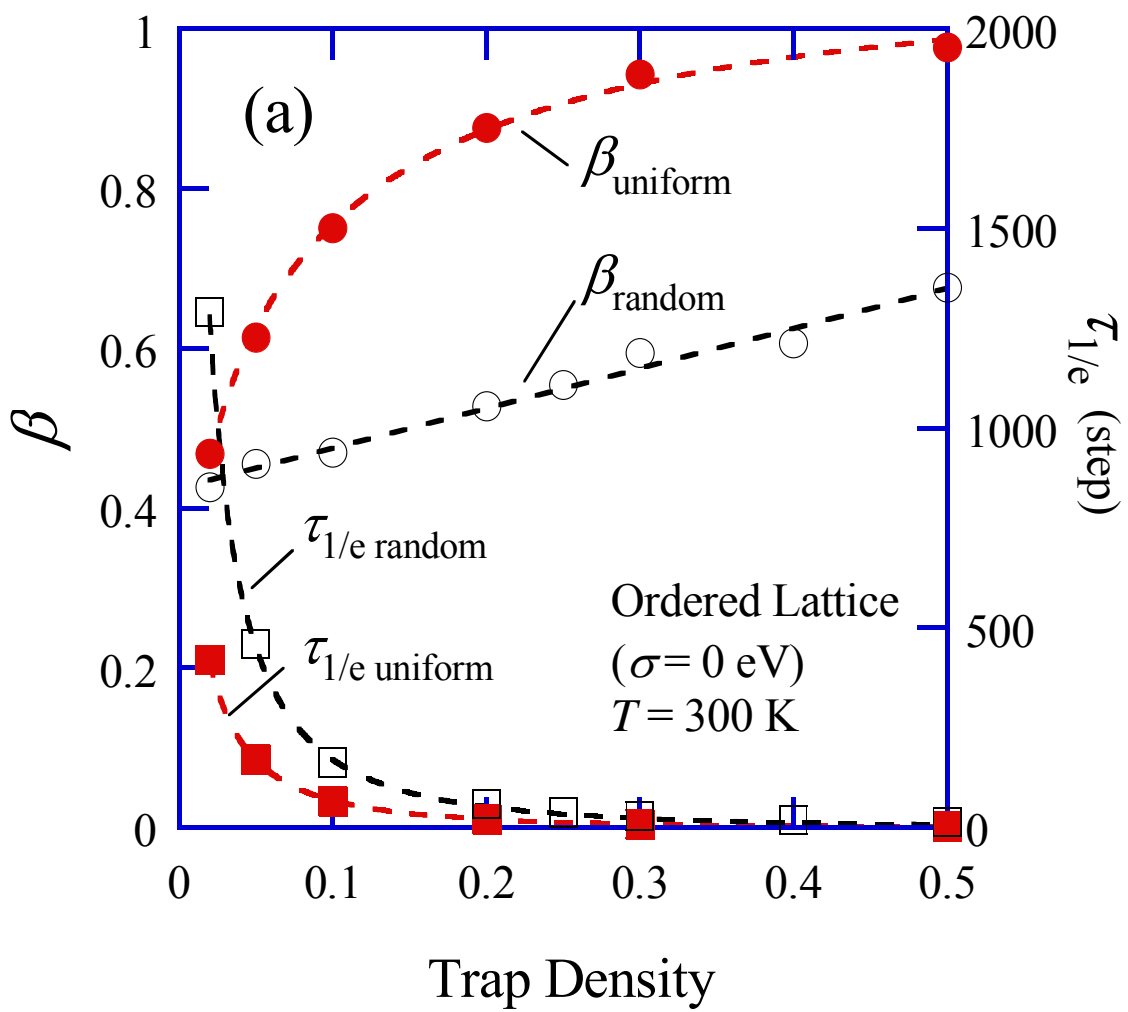


Fig. 3 (a)

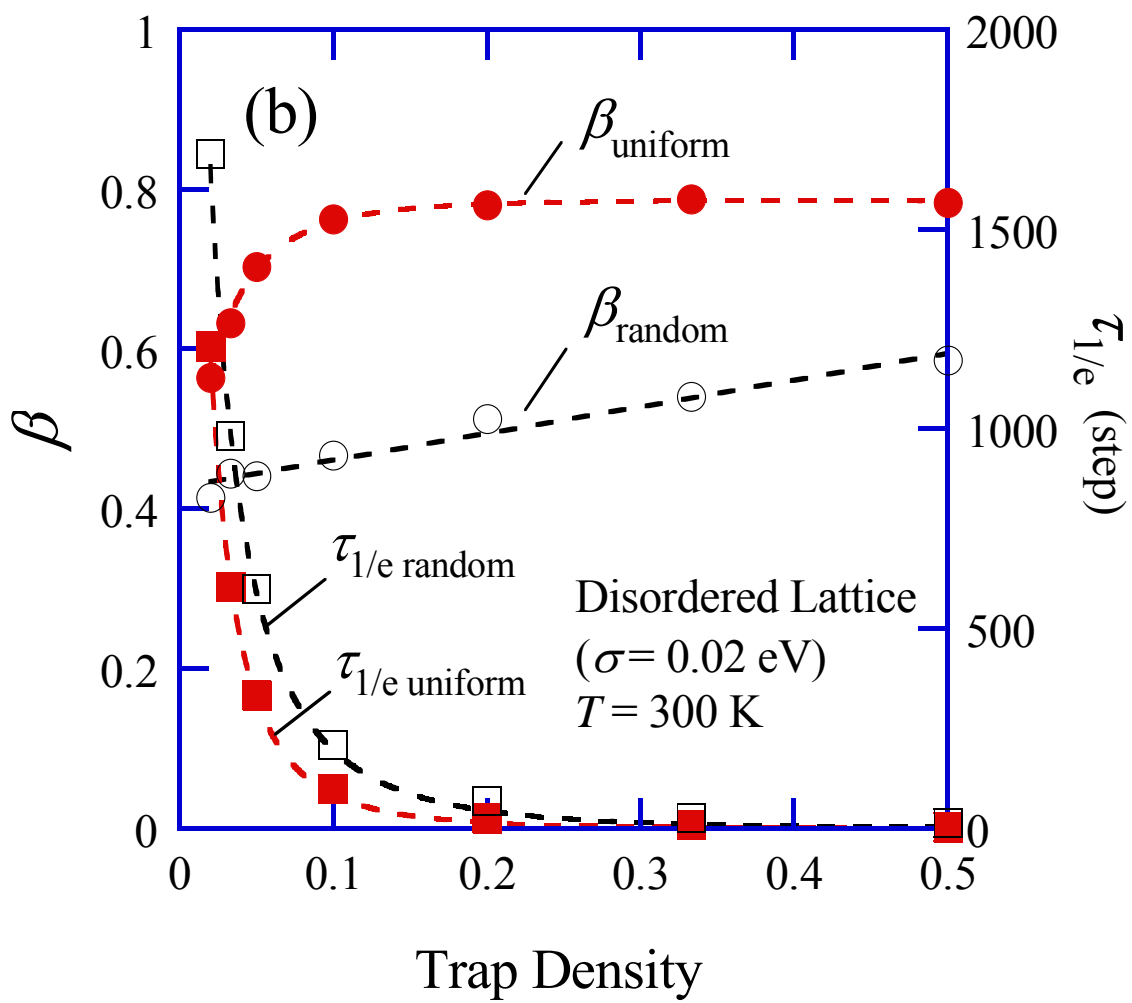


Fig. 3 (b)

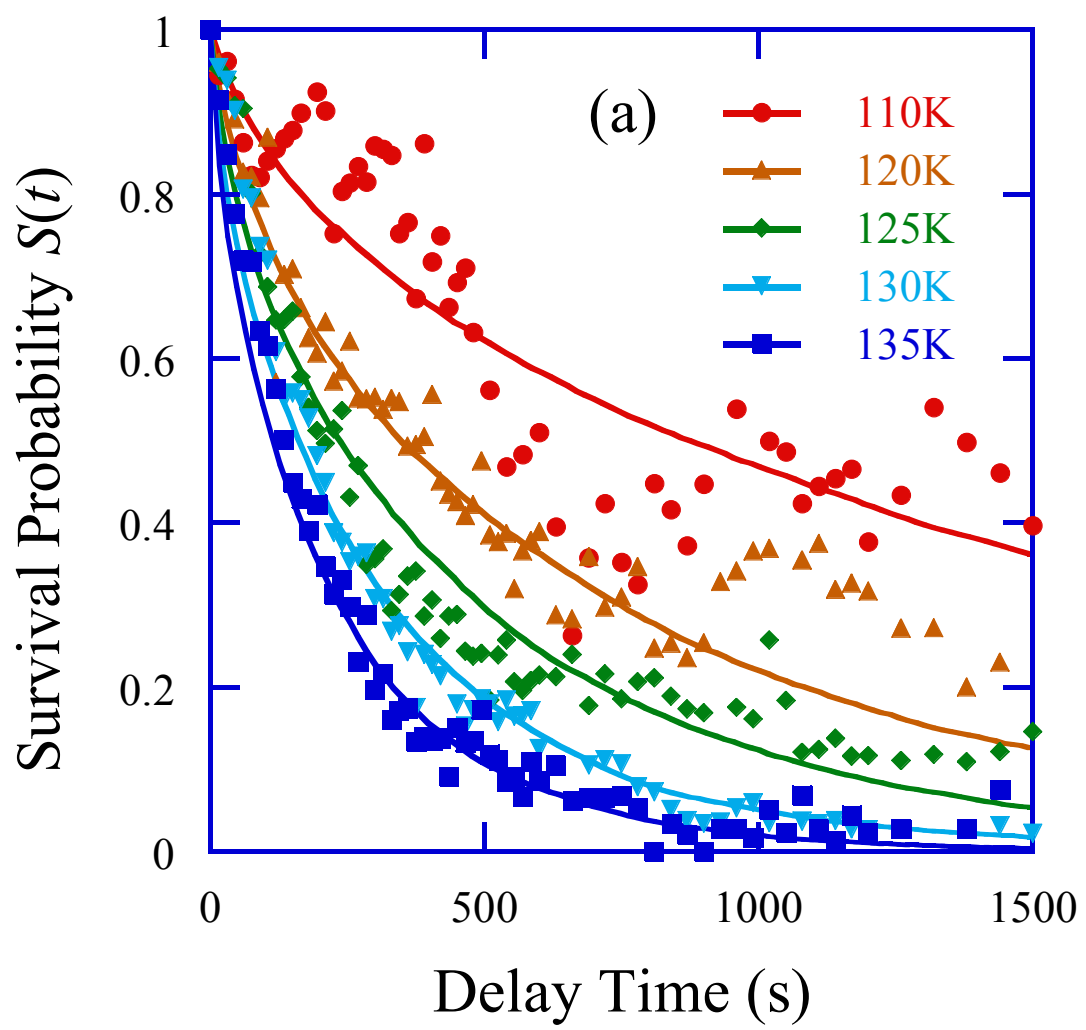


Fig. 4 (a)

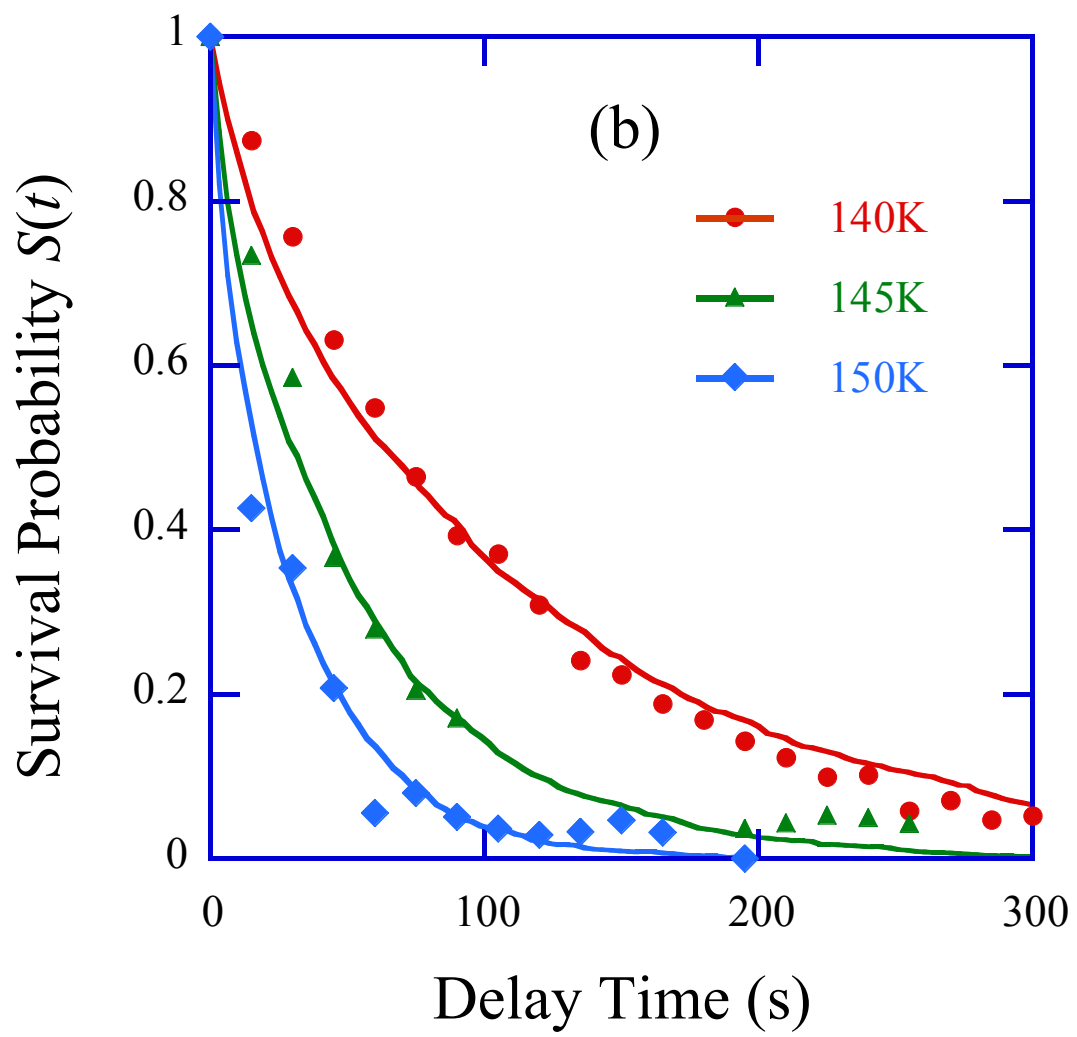


Fig. 4 (b)

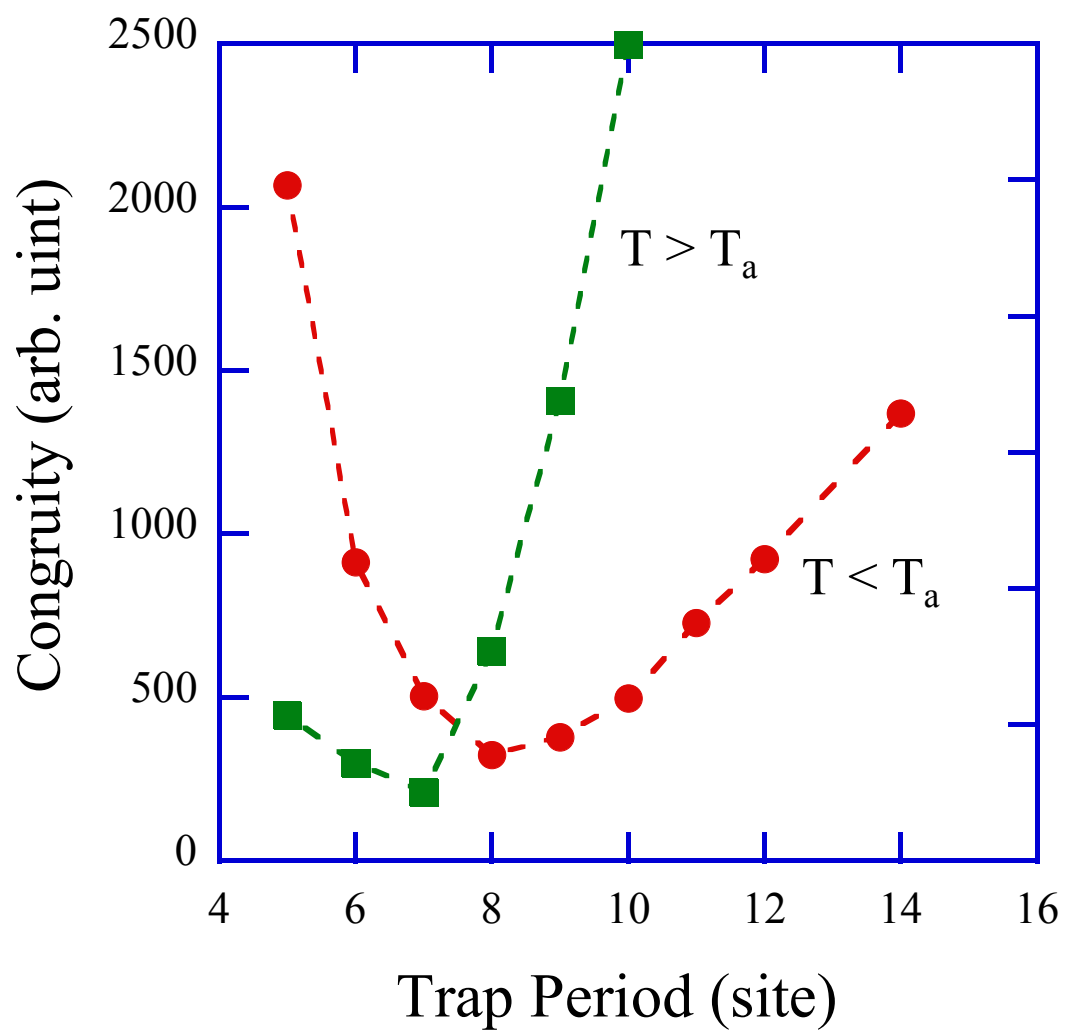


Fig. 5

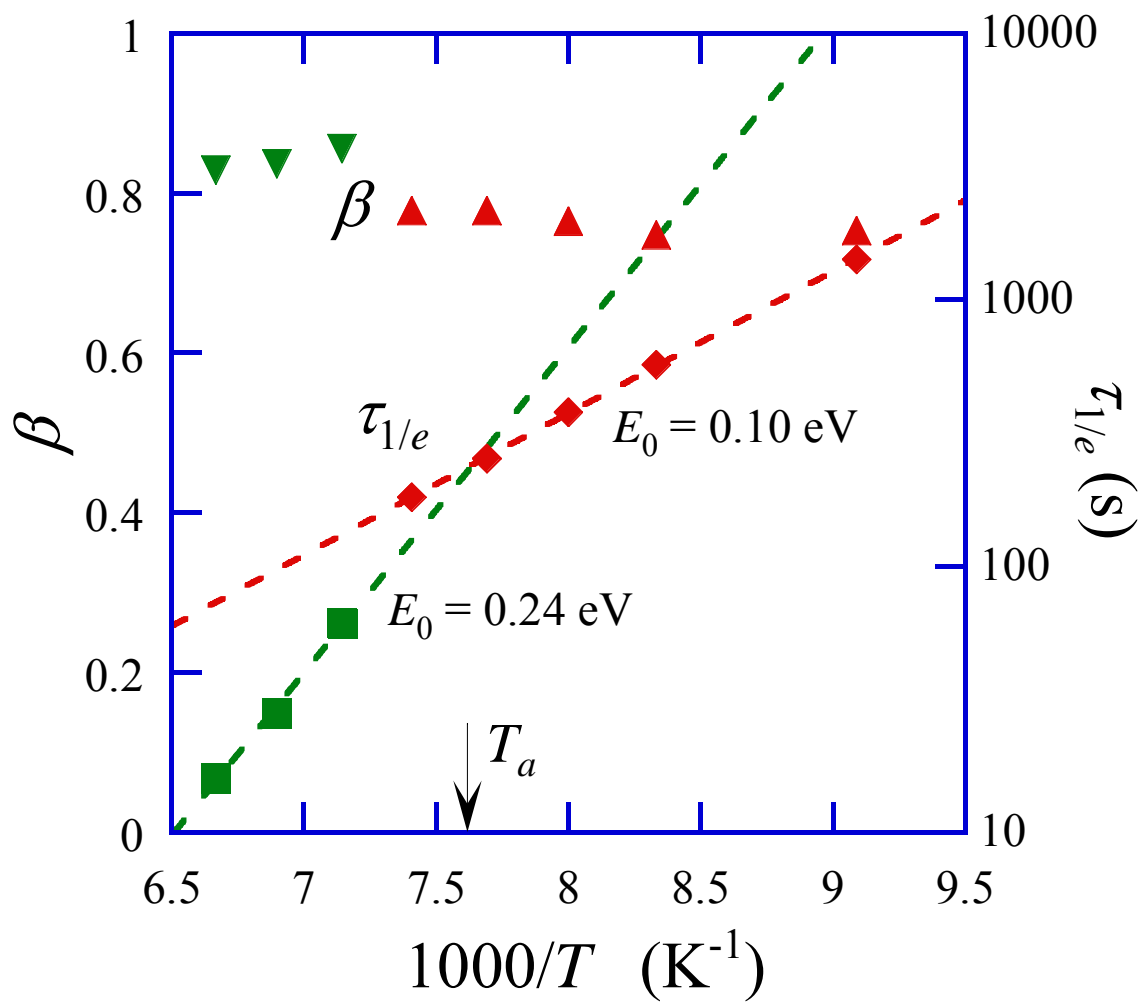


Fig. 6